Journal of Insect Science, (2020) 20(6): 31; 1–10
doi: 10.1093/jisesa/ieaa132
Research

Identification and Characterization of Aldehyde Oxidase 5 in the Pheromone Gland of the Silkworm (Lepidoptera: Bombycidae)

Yandi Zhang,[1,2] Yu Yang,[1,2] Guanwang Shen,[1,2,3,4] Xueqin Mao,[1,2] Mengyao Jiao,[1,2] and Ying Lin[1,2,3,4,5]

[1]State Key Laboratory of Silkworm Genome Biology, Southwest University, Chongqing, 400716, China, [2]Biological Science Research Center, Southwest University, Chongqing, 400716, China, [3]Chongqing Key Laboratory of Sericulture Science, Chongqing, 400716, China, [4]Chongqing Engineering and Technology Research Center for Novel Silk Materials, Chongqing, 400716, China, and [5]Corresponding author, e-mail: ly908@swu.edu.cn

Subject Editor: Russell Jurenka

Received 31 August 2020; Editorial decision 29 October 2020

Abstract

Aldehyde oxidases (AOXs) are a subfamily of cytosolic molybdo-flavoenzymes that play critical roles in the detoxification and degradation of chemicals. Active AOXs, such as AOX1 and AOX2, have been identified and functionally analyzed in insect antennae but are rarely reported in other tissues. This is the first study to isolate and characterize the cDNA that encodes aldehyde oxidase 5 (BmAOX5) in the pheromone gland (PG) of the silkworm, *Bombyx mori*. The size of *BmAOX5* cDNA is 3,741 nucleotides and includes an open reading frame, which encodes a protein of 1,246 amino acid residues. The theoretical molecular weight and isoelectric point of BmAOX5 are approximately 138 kDa and 5.58, respectively. BmAOX5 shares a similar primary structure with BmAOX1 and BmAOX2, containing two [2Fe-2S] redox centers, a FAD-binding domain, and a molybdenum cofactor (MoCo)-binding domain. RT–PCR revealed *BmAOX5* to be particularly highly expressed in the PG (including ovipositor) of the female silkworm moth, and the expression was further confirmed by in situ hybridization, AOX activity staining, and anti-BmAOX5 western blotting. Further, BmAOX5 was shown to metabolize aromatic aldehydes, such as benzaldehyde, salicylaldehyde, and vanillic aldehyde, and fatty aldehydes, such as heptaldehyde and propionaldehyde. The maximum reaction rate (V_{max}) of benzaldehyde as substrate was 21 mU and K_m was 1.745 mmol/liter. These results suggested that BmAOX5 in the PG could metabolize aldehydes in the cytoplasm for detoxification or participate in the degradation of aldehyde pheromone substances and odorant compounds to identify mating partners and locate suitable spawning sites.

Keywords: aldehyde oxidase, identification, activity staining, pheromone gland, *Bombyx mori*

Aldehyde oxidases (AOXs) belong to the family of molybdoenzymes (MEs) (Garattini et al. 2003), and MEs are structurally conserved proteins containing two identical 40~150 kDa catalytic subunits, depending on the enzyme (Garattini et al. 2008). The structure of each AOX monomer includes a 20 kDa N-terminal two [2Fe-2S] domains, a 40 kDa central domain containing a flavin adenine dinucleotide (FAD)-binding site, and an 85 kDa C-terminal substrate-binding catalytic domain with a molybdenum cofactor (MoCo) site (Garattini et al. 2003, Mahro et al. 2011). AOX domains are similar to those of xanthine oxidoreductase (XOR), which plays a key role in the catabolism of purines, metabolizing hypoxanthine into xanthine and xanthine into uric acid (Enroth et al. 2000). AOXs have broad substrate specificity, hydroxylating N-heterocycles or oxidizing aromatic and fatty aldehydes into their corresponding acids (Majkic-Singh et al. 1983, Mira et al. 1995, Kundu et al. 2007). The significance of AOX in drug metabolism has been increasingly highlighted in the past few years (Pryde et al. 2010). In addition, AOX catalyzes the reduction of a variety of functional groups, including sulfoxides, N-oxides, azo dyes, and N-hydroxycarbamoyl substituents in the presences of an appropriate donor. In addition, N-heterocyclic drugs such as methotrexate, 6-mercaptopurine, cinchona alkaloids, and famciclovir are oxidized by AOX (Obach et al. 2004, Kitamura et al. 2006). Importantly, AOX oxidizes electrophilic carbons of azaheterocycle scaffolds, such as pyridine, pyrimidine, and pyridazine, which are often included in therapeutic drugs to increase solubility (Garattini and Terao 2013, Hutzler et al. 2013). However, the physiological function of these enzymes remains largely undefined.

In insects, pheromones are metabolized by antennal AOX and have been confirmed at the molecular level (Rybczynski et al. 1989,

Choo et al. 2013). Antennae-specific AOX in *Manduca sexta*, *Antheraea polyphemus*, and *Bombyx mori* can degrade aldehydic sex pheromones, such as bombykal (Rybczynski et al. 1989, Rybczynski et al. 1990). Some researchers have reported that AOX is related to insecticide resistance in *Culex quinquefasciatus* because *AOX* is coamplified with insecticide resistance-associated esterases (Hemingway et al. 2000). The first insect antennal AOX was cloned from the cabbage armyworm *Mamestra brassicae* (Merlin et al. 2005). Recently, one antenna-specific AOX gene (*AtraAOX2*) was also cloned from navel orangeworm *Amyelois transitella* (Choo et al. 2013). In the common fruit fly, *Drosophila melanogaster*, four *AOX* genes with different expression patterns have been identified and analyzed, of which three genes encode active AOX proteins and metabolize different specific substrates (Marelja et al. 2014). Six putative AOX genes (*HarmAOX1-6*) were identified in the cotton bollworm, *Helicoverpa armigera*; *HarmAOX1* is highly expressed in adult antennae, as well as tarsi and larval mouthparts, whereas *HarmAOX2* is highly and specifically expressed in adult antennae (Xu and Liao 2017). So far, mainly AOX1 and AOX2 have been reported to be involved in the degradation of pheromone components in the antennae. However, activity identification and characterization studies of other AOXs have been rarely conducted in insects.

The silkworm *B. mori* is a lepidoptera model insect. In addition, silkworm genome sequences have been well characterized (Xia et al. 2004), thus further improving research utilizing this species. The past decade has witnessed the cloning and molecular characterization of antenna-specific AOX genes *BmAOX1* and *BmAOX2* (Rybczynski et al. 1990). Recently, eight *AOX*s were found in the silkworm genome by known *AOXs* BLAST search against the Silkworm Genome Database (Pelletier et al. 2007, Yang et al. 2010). We previously noted transcript expression of eight *BmAOXs* in different tissues of female silkworm pupa or moths, and we found high, specific expression of *BmAOX5* in the pheromone gland (PG) of female silkworm moths (Yang et al. 2010). In 2019, BmIAO1 was identified in the silkworm silk gland of silkworms, which is involved in indole-3-acetic acid synthesis (Takei et al. 2019). Although eight *BmAOXs* are expressed in the silkworm, only active BmAOX1 and BmAOX2 have been identified in the antennae, which are speculated to be involved in the oxidization of bombykal (Pelletier et al. 2007). Active BmIAO1 has been identified in the silk gland, but active AOXs have not been identified in the PG. In a previous study, *BmAOX5* was found to be specifically and highly expressed in the PG at the silkworm moth stage; however, its ability to synthesize active AOX is unclear. The expression localization and function of BmAOX5 in silkworm PG are still unknown.

This study focused on the cloning, expression, localization, and enzyme activity analysis of *BmAOX5* in the silkworm PG. The results of this study will help improve our understanding of the complex function of AOXs and lay the foundation for lepidoptera insect defense research and development of an insect medication model.

Materials and Methods

Insect and Sample Preparation

Bombyx mori dazao strain was maintained at the State Key Laboratory of Silkworm Genome Biology in Southwest University (Chongqing, China). Larvae were reared on fresh mulberry leaves (*Morus sp.*) at 25 ± 2°C; pupae and moth were maintained at 25°C. The head and antennae, thorax and wings, abdomen, fat body, ovaries, and PG (including ovipositor) at late pupa and moth stages were dissected from females and collected in different 1.5 ml Eppendorf tubes. Tissues were rapidly frozen using liquid N_2 and stored at −80°C until further use. All the powders were made by grinding the samples in liquid N_2 immersion. Different sample (200 mg) was collected in different 1.5 ml Eppendorf tube. The samples selected for protein analysis were supplemented with 1 ml of lysis buffer (0.1 mol/liter Tris–HCl, pH 8.0, 100 µmol/liter EDTA, 1 mmol/liter DTT, and 2× protease inhibitor cocktail [Roche, Basel, Switzerland]), and homogenization was performed for 30 min at 4°C. The crude extract was centrifuged at 14,000 *g* for 30 min at 4°C; the supernatant of each sample was then transferred to a clean 1.5 ml Eppendorf tube for AOX activity and western blotting analysis.

Total RNA Extraction and cDNA Synthesis

Total RNA from the different tissues of female silkworms were extracted using TRIzol reagent (Invitrogen, Carlsbad, CA) and treated with DNase I (Promega, Madison, WI). For reverse-transcription polymerase chain reaction (RT–PCR), single-stranded cDNA was synthesized from total RNA (4 µg) using the M-MLV reverse transcriptase reference protocol supplied with the Advantage RT for PCR Kit (Clontech Laboratories Inc., Mountain View, CA). To obtain the complete cDNA sequence of *BmAOX5*, PG cDNA was synthesized from female silkworm PG total RNA (2 µg) at 42°C for 1.5 h using the SMART RACE cDNA Amplification Kit (Clontech Laboratories, Inc.) with Superscript II reverse transcriptase (Gibco Waltham, MA), predicted 5′-or 3′-*BmAOX5* coding sequence (CDS) primers, and SMART II oligonucleotide (Clontech Laboratories Inc.) according to the manufacturer's instructions.

Cloning and Sequence Analysis

The CDS of BmAOX5 was downloaded from the Silkworm Genome Database SilkDB v2.0 (http://silkworm.genomics.org.cn) (Duan et al. 2010). We designed primers (*BmAOX5-AF*: 5′-CGCTAAATGCGTACATCAGA-3′, *BmAOX5-AR*: 5′-GCAATC TTCAAGCGACACG-3′; *BmAOX5-BF*:5′-GAGGGCGTGGATTC TTAT-3′, *BmAOX5-BR*: 5′-CAGAGGTGGTGAAGACAAA-3′) for segmented PCR amplification of *BmAOX5* in PG cDNA of silkworm moths on day 1 after mating without egg laying. The following condition were used for PCR: predenaturation at 94°C for 5 min, 30 cycles of denaturation at 94°C for 50 s, annealing at 62°C for 40 s, extension at 72°C for 1 min, and final extension at 72°C for 10 min. The obtained fragments were cloned in pMD18-T vectors (TaKaRa Bio, Kusatsu, Japan) and sequenced by the Beijing Genomics Institute (BGI, Beijing, China). Sequences of *BmAOX5* were aligned and spliced for complete *BmAOX5* cDNA using BioEdit Sequence Alignment Editor (BioEdit Version 7.2.5) (Hall 1999). The protein sequences of BmAOX5 were translated using the Expasy-translate tool (https://web.expasy.org/translate/). The theoretical molecular weight and isoelectric point of the BmAOX5 protein were calculated using Compute pI/Mw software (https://web.expasy.org/cgi-bin/ compute_pi/pi_tool), and the signal peptide of BmAOX was analyzed using SignalP 4.0 (Petersen et al. 2011). Amino acid sequences of BmAOX1, BmAOX2, BmXDH1, and BmXDH2 were obtained from NCBI (www.ncbi.nlm.nih.gov) and were aligned using the BioEdit Sequence Alignment Editor (BioEdit Version 7.2.5) (Hall 1999).

Expression and RT–PCR Detection of *BmAOX5*

Based on the complete cDNA of *BmAOX5*, we designed the prokaryotic expression primers for the complete BmAOX5 CDS for PCR amplification using the PG cDNA of silkworm moths sampled

on day 1 after mating but before egg laying: *pET-BmAOX5-F*:5′-CGC*GGATCC*ATGTCGCTAAATGCGTACATCAGA-3′, *pET-BmAOX5-R*:5′-CG*AGCTC*TTACTAGTCAGAGGTGGTGAAGA CAAAC-3′ (the italics bases with represent BamH I and Sac I restriction sites, respectively). The PCR conditions were as follows: predenaturation at 95°C for 4 min, 30 cycles of denaturation at 95°C for 30 s, annealing at 68°C for 30 s, extension at 72°C for 3 min, and final extension at 72°C for 10 min. The obtained fragments were cloned in pET 28a vectors (TransGen Biotech, Beijing, China) and sequenced by the Beijing Genomics Institute (BGI). The fragment was then transformed into competent *Escherichia coli.* BL21 (*DE3*) cells (TransGen Biotech, Beijing, China), and expression was induced using 0.2 mmol/liter IPTG (Takara Bio) at 16°C according to the manufacturer's instructions. Protein induced was used as an antigen to verify the antibody of BmAOX5.

Primers (*BmAOX5F*: 5′-AAAGGCACGGATGTAA-3′; *BmAOX5R*: 5′-TGTAGCGGTATTCAGG-3′) designed for RT–PCR were situated between 2019 bp and 2544 bp in *BmAOX5* CDS. *Actin-related protein 3* gene was used as a control for assessing cDNA integrity (*BmActin3-F*: 5′-AACACCCCGTCCTGCT CACTG-3′; *BmActin3-R*: 5′-GGGCGAGACGTGTGATTTCCT-3′). PCR was performed using rTaq DNA polymerase (Promega) and 1 µl of cDNA, according to the manufacturer's instructions. The PCR conditions used were as follows: predenaturation at 94°C for 5 min, 25 cycles of denaturation at 94°C for 30 s, annealing at 58°C (*BmAOX5*)/53°C (*Actin3*) for 30 s, extension at 72°C for 1 min, and final extension at 72°C for 10 min. PCR products were loaded onto 1.5% agarose gel for detection by gel electrophoresis.

In Situ Hybridization of Silkworm Moth PG

The BmAOX5 cDNA fragment was cloned in the pMD19 T vector (TaKaRa Bio) and used as a template for synthesis of sense and antisense riboprobes using T7 RNA polymerases in the DIG RNA Labeling Kit (Roche). The primers were located between 247 bp and 684 bp, *BmAOX5-antisense-F*: 5′-ACGGCCATAGCCCGATGTT-3′, *BmAOX5-antisense-R:* 5′-*GTAATACGACTCACTATAGGGAGA* CGATTCCTTCGCAAGCACC-3′ *BmAOX5-sense-F*: 5′-*GTAAT ACGACTCACTATAGGGAGA*ACGGCCATAGCCCGATGTT-3′; *BmAOX5-sense-R*: 5′-CGATTCCTTCGCAAGCACC-3′ (the italics bases represent T7 promoter sequences). Template DNA was degraded using DNase I (Promega). The PG of silkworm moths collected on day 1 after mating without egg laying were fixed in 4% (w/v) paraformaldehyde for 4 h at 4°C, embedded in paraffin, sectioned to 5 µm thickness using a slicing machine (Leica Rm 2235, Germany), and mounted onto chromalum-containing gelatin-coated slides. The conditions for slide, pretreatment, hybridization, washing, and detection by nuclear-track emulsion were described previously (Kurosaki et al. 1996). At the end of the in situ hybridization, tissue sections were stained using nitro blue tetrazolium/5-bromo-4-chloro-3-indolyl phosphate solution (Roche) and photographed under a BX53 microscope (Olympus America Inc.).

AOX Activity Staining Analysis

AOX activity in the PG, antenna, and ovary extracts of the female silkworm moths sampled on day 1 without mating were measured as described by Rybezynski et al. (1989). Total proteins (40 µg) in each lane were separated using 8% native-PAGE, and the gels were subsequently stained for AOX activity using 5 mmol/liter AOX substrate, such as benzaldehyde (Sigma), heptaldehyde (Sigma), salicylaldehyde (J&K Chemical Ltd. Shanghai, China), propionaldehyde (J&K), and vanillic aldehyde (J&K), with 0.4 mmol/liter 3-(4,5-dimethylthiazolyl-2)-2,5-diphenyltetrazoliumbromide (MTT) and 0.1 mmol/liter phenazine methosulfate (PMS) as the electron acceptors. Upon AOX reaction, the reducing agent precipitated with a purple color, making the blue band visible in the native gel (Marelja et al. 2014).

BmAOX5 Protein Detection

For western blotting analysis, the native-PAGE and SDS–PAGE gels were prepared according to a previously described method (Laemmli 1970), and were then stained with Quick Coomassie brilliant blue (CBB) (Wako, Osaka, Japan) or transferred into polyvinylidene fluoride (PVDF) membranes (Roch) under 1.0 mA for 30 min. The PVDF membrane was then blocked in 3% Tris-buffered saline and Tween 20 (TBST) skim milk for 1 h at 4°C, followed by incubation with anti-BmAOX5 primary antibody (1:2,000, synthesized using an immunized rabbit treated with BmAOX5-special polypeptides [amino acid positions 33–45, RAKRYPSGKTETF], Genscript Nanjing Co. Ltd.) in 3% TBST skim milk for 1 h at room temperature (RT, about 25°C). The membrane was washed 5× with TBST for 5 min in a rotary shaker and incubated with the secondary antibody of horseradish peroxidase-conjugated goat anti-rabbit IgG (1:10,000; Sigma–Aldrich, St. Louis, MO) in 3% TBST skim milk for 1 h at RT. The membrane was washed 3× with TBST for 10 min in a rotary shaker and then incubated with the chemiluminescent substrate from the ECL Plus Western Detection Kit (GE Healthcare, Chicago, IL) for 5 min and photographed using a Clinx ChemiScope 3400 Mini (Science Instrument, Beijing, China).

Activity Analysis of BmAOX5 Enzyme

BmAOX5 activity was measured by incubating the PG extracts of frozen silkworm moths collected on day 1 without mating for 5 min initiating the reaction with a substrate solution (0.1 mol/liter potassium phosphate buffer, pH 8; 0.1 mmol/liter PMS; 0.4 mmol/liter MTT; and AOX substrate). The concentration of PG extracts was 20 µg/µl as measured using the BCA protein determination method. PG extracts (30 µl equivalent to 600 g of total protein) was added to the substrate solution, and BmAOX5 activity was evaluated based on the formation of insoluble purple formazan (Rothe 1974) at 560 nm (Alirezaei et al. 2008). One OD/min was representative of 1 unit of enzyme activity (1 U) in the catalytic reaction process. We employed the following concentrations of benzaldehyde (Sigma) as substrate: 1, 1.3, 1.6, 2, 2.5, 3.5, 5, 6, 8, and 10 mmol/liter. Each concentration was analyzed in triplicate. Samples lacking PG protein extracts were used as blank controls to adjust for nonenzymatic background activity.

Results

Cloning and Structural Analysis of the *BmAOX5*

In our previous study, *BmAOX5* was found to be specifically and highly expressed in the PG of silkworm moths. As there were no reports concerning the complete CDS of *BmAOX5* or its structure or studies targeting this gene, we first cloned the gene cDNA of *BmAOX5*. Based on the predicted CDS of *BmAOX5* from the silkworm genome database SilkDB v2.0, we cloned and analyzed *BmAOX5*. The complete CDS of *BmAOX5* revealed a length of 3,741 nucleotides (GenBank accession number KY643683), encoding a BmAOX5 protein (GenBank accession number AQY62686) with 1,246 amino acid residues lacking the signal peptide. The theoretical molecular weight and isoelectric point of BmAOX5 were approximately 138 kDa and 5.58,

respectively. Multiple sequence alignment showed that BmAOX5 had homology with BmAOX1 and BmAOX2, with 44% amino acid identity; BmXDH1 and BmXDH2 had 43% and 41% amino acid identity with BmAOX5, respectively. BmAOX5 has some conserved domains containing common features consistent with antennae-specific BmAOX1 and BmAOX2 in the silkworm (Terao et al. 2001). These conserved domains of the BmAOX5 had two [2Fe-2S] redox centers, a FAD-binding domain, and a MoCo-binding domain, as shown in Fig. 1. Unlike XOR proteins, such as BmXDH1 and BmXDH2, BmAOX5 protein did not require NAD^+ as a cofactor for their catalytic activity because it lacks some amino acid residues (black box in Fig. 1), which are responsible for binding NAD^+ (Terao et al. 2009) such as amino acid sequence FFTGYRKTIVKPE in chicken XOR (Johnson et al. 1985). The NAD^+-binding sequence was well conserved in all XOR proteins but was missing in AOXs. These results revealed that BmAOX5 belongs to a subfamily of cytosolic molybdo-flavoenzymes, AOXs.

Expression and Localization of BmAOX5 in the PG of Silkworm

Silkworm PG is located between the eighth and ninth abdominal segments and functions in synthesizing sex pheromones. BLAST search of *BmAOX5* in the SilkDB2.0 revealed that *BmAOX5* is highly expressed in the moth stage (data unpublished). We detected the expression of *BmAOX5* in different tissues of female silkworm moths and found *BmAOX5* to be especially highly expressed in the PG (Fig. 2A). RT–PCR further detected the expression patterns of *BmAOX5* in silkworm PG at different developmental stages. These results indicated that *BmAOX5* is most highly expressed in female silkworm moths after mating without egg laying and is also highly expressed after mating and laying eggs (Fig. 2B). *BmAOX5* was also expressed in nonmating female silkworm moths and late-stage pupa (Fig. 2B). We selected the PG of female silkworm moth day 1 after mating without egg laying for in situ hybridization. The anatomy of the female silkworm moth tail clearly showed a pair of colorless eversible ventrolateral sacs, which were identified as PG (Fig. 2C, shown by the red arrow) (Fonagy et al. 2001). In situ hybridization revealed the presence of the probe signal of antisense *BmAOX5* RNA in the capsule wall of the PG and the inner wall of the oviposition tube (Fig. 2D). These results suggest that BmAOX5 may play a role in aldehyde pheromone or odorant compound degradation and concentration adjustment.

Activity Identification of BmAOX5 in Silkworm PG

PG proteins of female silkworm pupae and moths in different stages were analyzed using native-PAGE, and then AOX activity staining was carried out using the common AOX substrates, benzaldehyde. The blue band shown in Fig. 3A indicates the activity of AOX proteins in each sample. The PGs of pupa from day 7 and moths from day 3 without mating demonstrated low AOX activity, whereas those from other stages exhibited activity bands, with the strongest activity band in moths from day 1 without mating. We then analyzed PG and antennae of female silkworm moths from day 1 without mating using AOX activity staining. One activity band was observed in the PG extracts, which differed from that in antenna extracts, indicating the band does not correspond to BmAOX1 or BmAOX2 protein. Further, AOX in the PG was unstable: AOX activity was almost lost after the PG extracts were stored at 4°C for 24 h, whereas AOX activity in the antenna extracts was stable (Fig. 3B). Therefore, the fresh extracts of frozen tissues were selected as experimental samples for the following experiments.

BmAOX5 was expressed specifically in the PG of female silkworm pupae and moths, but it was unknown whether AOX activity in the PG was produced by BmAOX5. To obtain further information regarding novel proteins in the silkworm PG, we first developed BmAOX5-specific antibodies by immunizing rabbits with selected BmAOX5 specific polypeptides (amino acid sequence RAKRYPSGKTETF, located at 33–45 aa). CBB staining results showed that BmAOX5 and another BmAOX were successfully overexpressed in *E. coli* (Fig. 3C, black arrow). BmAOX5 antibodies could detect an ~140 kDa protein band in extracts of *E. coli* with overexpressed BmAOX5 but could not detect BmAOX5 in extracts of *E. coli* transformed with the corresponding empty vector (pET28a) and another *BmAOX* gene (Fig. 3D, black arrow). These results indicated anti-BmAOX5 could specifically recognize BmAOX5 proteins.

To identify which AOX protein corresponded to the protein activity observed in the PG, native-PAGE was performed using PG extracts of moths from day 1 without mating and ovary extracts as the control. Part of the native-PAGE gel was analyzed using AOX activity staining toward benzaldehyde (Fig. 3E, black arrow), whereas the other part of the gel was analyzed by western blotting (Fig. 3F, black arrow). The migration rate of one band in the activity staining gel was consistent with the western blotting results of PG extracts (Fig. 3E and F), which suggested that BmAOX5 corresponded to the activity band. The results revealed that *BmAOX5* could transcript and translate into active AOX protein in the female silkworm moth PG.

Activity of BmAOX5 With Different Substrates

To characterize BmAOX5 activity, we compared the enzyme activity of BmAOX5 using aromatic aldehydes such as benzaldehyde, salicylaldehyde, and vanillic aldehyde, and fatty aldehydes such as heptaldehyde and propionaldehyde as substrates. First, PG protein extracts of silkworm moths 1 d without mating were subjected to native-PAGE followed by AOX activity staining (Fig. 4A). One activity band was observed in protein extracts of frozen silkworm moth PG when benzaldehyde was used as the substrate; however two strong activity bands were observed in protein extracts of fresh silkworm moth PG. This suggested that either BmAOX5 had two forms or another type of BmAOX was present in silkworm moth PG. Two strong activity bands were also observed in the gel using salicylaldehyde as a substrate for protein extracts of fresh silkworm moth PG. Two activity bands with very weak signals were observed using vanillic aldehyde as a substrate. When heptaldehyde was used as the substrate, one strong activity band and another weak activity band were observed. One strong and one very weak activity bands were observed when propionaldehyde was used as a substrate. These results indicate that BmAOX5 can metabolize aromatic and fatty aldehydes.

According to previous experimental results, we conducted kinetic analysis of BmAOX5 enzymatic reaction with the different concentrations benzaldehyde as substrate using fresh extracts of the frozen silkworm moth PG. Based on the relationship between substrate concentration and reaction rate, a substrate saturation curve for the enzymatic reaction was prepared (Fig. 4B). We found that reaction rate increased in association with increasing substrate concentration, and reaction rate increased slightly when substrate concentration exceeded 8 mmol/liter. Double reciprocal plotting of reaction rate and substrate concentration data showed that the plot met the requirements of the Michaelis equation (Fig. 4C). The maximum reaction rate (V_{max}) was 21 mU, and the K_m was 1.745 mmol/liter. The results showed BmAOX5 has typical characteristics of enzyme activity. This suggested BmAOX5 is involved in the degradation of aldehydes in the silkworm PG.

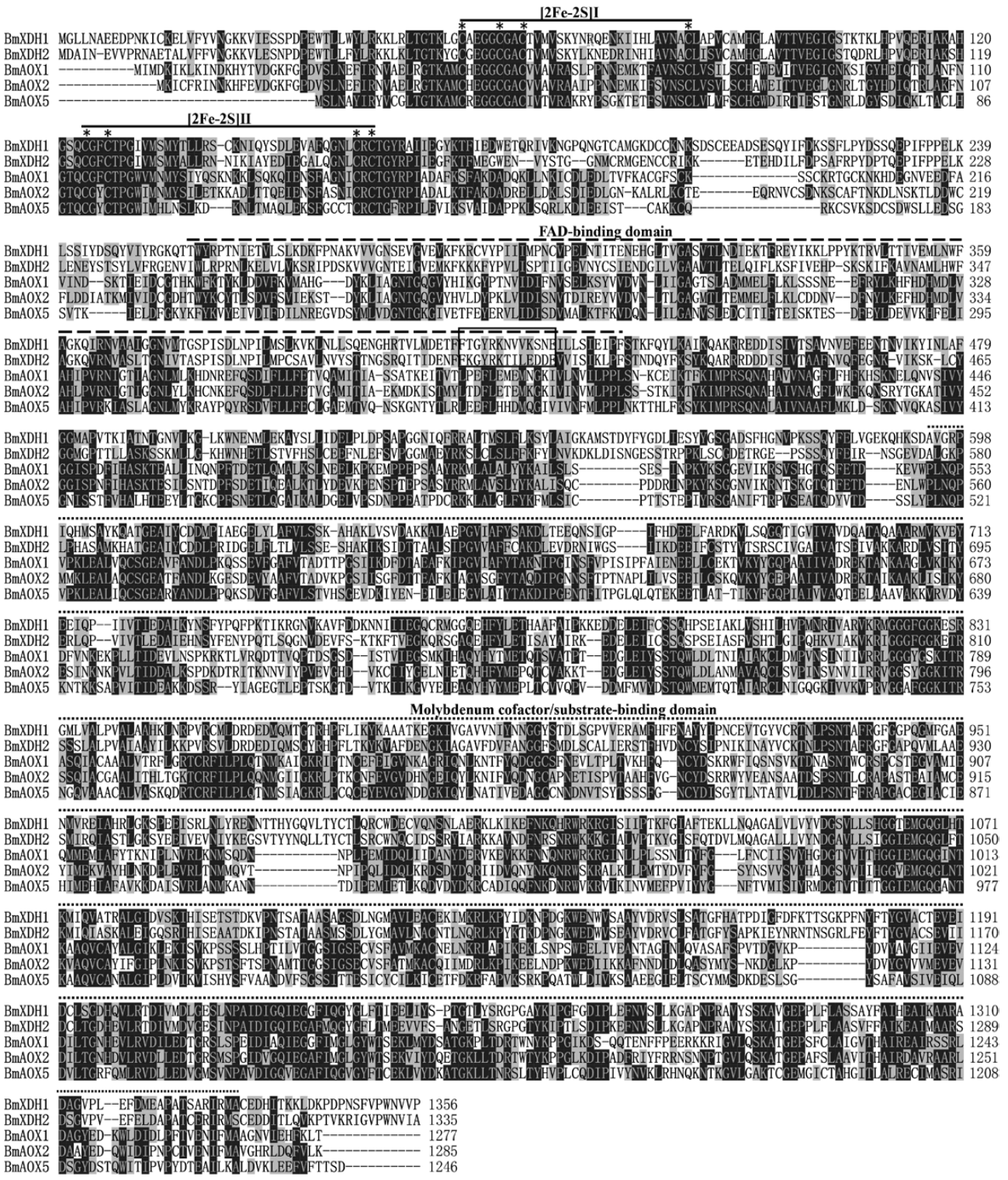

Fig. 1. Sequence alignment analysis of BmAOX5. Overline, [2Fe-2S] redox centers. *, Cysteine residues. Short overline, FAD-binding domain. Dashed overline, MoCo-binding domain. The NAD-binding site typical of XDHs is boxed. The background color of identical residues is black; the background color of positive residues is light gray; the background color of no positive residues is white. BmAOX1, *B. mori* aldehyde oxidase 1 (NP_001103812); BmAOX2, *B. mori* aldehyde oxidase 2 (NP_001103811); BmXDH1, *B. mori* xanthine dehydrogenase 1 (BAA21640); BmXDH2, *B. mori* xanthine dehydrogenase 2 (BAA24290); BmAOX5, *B. mori* aldehyde oxidase 5 (AQY62686).

Discussion

In this study, we report the identification and characterization of a novel member of the molybdo-flavoprotein family, BmAOX5. For the first time, cDNA of BmAOX5 from the silkworm PG was cloned and sequenced, whose encoded protein shared a striking resemblance with other AOXs, containing two [2Fe-2S] domains, a FAD-binding domain, and a MoCo-binding domain. Tissue distribution of BmAOX5 indicated that it was highly and specifically expressed

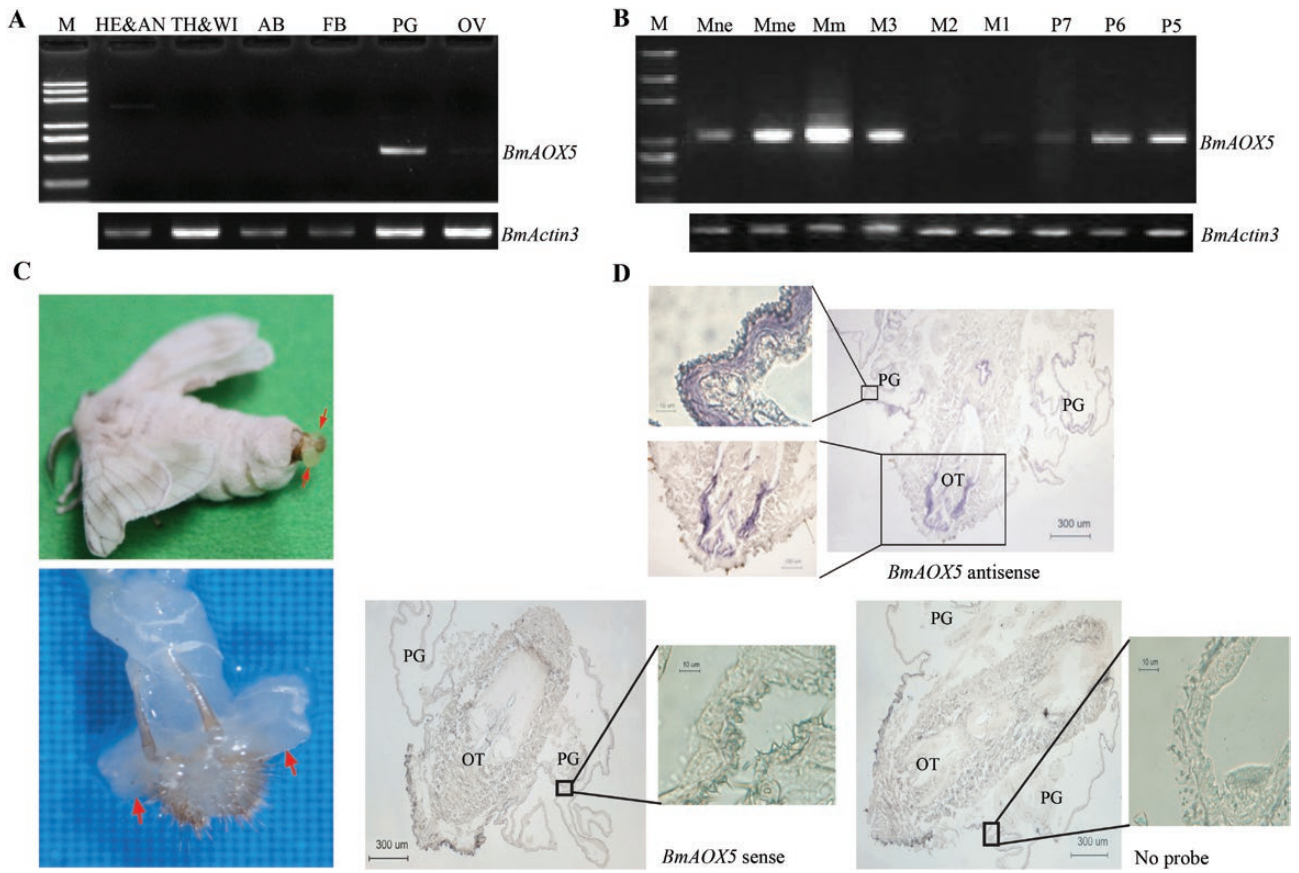

Fig. 2. Analysis of *BmAOX5* expression and localization in the PG of silkworm. (A) Transcription patterns of *BmAOX5* detected in female silkworm moth tissues by RT–PCR. M, DL2000; HE & AN, head and antennae; TH & WI, thorax and wings; AB, abdomen; FB, fat body; PG, pheromone gland with ovipositor; OV, ovaries (B) Expression patterns of *BmAOX5* detected in the PG during different stages by RT–PCR. M, DL2000; Mne, moth after egg laying without mating; Mme, moth after egg laying with mating; Mm, moth after mating without egg laying; M3, moth day 3 without mating; M2, moth day 2 without mating; M1, moth day 1 without mating; P7, pupa day 7; P6, pupa day 6; P5, pupa day 5. Amplification of the *BmActin3* gene was used as an endogenous control. (C) Anatomy of the female silkworm moth. Red arrow indicates the PG. (D) Localization of *BmAOX5* transcripts were detected in the PG by in situ hybridization. No RNA probes and *BmAOX5* sense RNA probes were used as controls for *BmAOX5* ant-sense RNA probes. Scale bar = 300 μm. OT, oviposition tube.

in the PG of female silkworm moth, and located in the PG capsule wall and the inner wall of the oviposition tube. BmAOX5 from silkworm PG can metabolize aromatic aldehydes, such as benzaldehyde, salicylaldehyde, and vanillic aldehyde, and fatty aldehydes, such as heptaldehyde and propionaldehyde. And its Vmax of benzaldehyde as substrate was 21 mU, and K_m was 1.745 mmol/liter.

Although BmAOX5 was expressed using a bacterial expression system, it did not exhibit AOX activity (data unpublished). BmAOX5 may thus differ from other AOX proteins (Alfaro et al. 2009, Marelja et al. 2014). We also attempted to purify BmAOX5 from the silkworm PG by benzamidine agarose gel affinity chromatography, which was reportedly employed to purify mammalian AOX (Terao et al. 2001, Terao et al. 2009); however, the results demonstrated that BmAOX5 is unstable. BmAOX5 enzyme activity was undetectable in the PG extracts stored at 4°C and −80°C for 24 h (data unpublished). Therefore, we employed fresh extracts of frozen PG to confirm active AOX as BmAOX5 through AOX activity staining and anti-BmAOX5 western blotting. Using these methods, we were able to detect active AOX in insect PG for the first time.

Owing to difficulties with AOX purification and instability, many researchers have measured mammalian AOX kinetics using liver cytosol, which exhibits AOX activity (Johnson et al. 1985, Strelevitz et al. 2012, Crouch et al. 2016). Human liver cytosol has been used to investigate drug metabolism mediated by AOX in vitro and to measure the influence of some inhibitors (Obach et al. 2004, Dalvie et al. 2010). Therefore, we adopted similar methods to conduct BmAOX5 kinetics experiments using silkworm PG cytosol. According to previous studies (Pryde et al. 2010, Hutzler et al. 2013), we selected five aldehydes as specific substrates for AOX catalysis and hypoxanthine as the specific substrate for xanthine oxidase (XOR), as the control. Benzaldehyde, salicylaldehyde, and vanillic aldehyde are aromatic aldehydes and excellent substrates for AOX that exhibit lower affinities with XOR (Panoutsopoulos and Beedham 2004, Marelja et al. 2014). Benzaldehyde and vanillic aldehyde have often been used as substrates for AOX activity detection in mammals. The fatty aldehydes heptaldehyde and propionaldehyde were also used as substrates for AOX activity analysis (Badwey et al. 1981, Walker-Simmons et al. 1989). In this study, native-PAGE and AOX activity staining assays indicated that BmAOX5 can metabolize a variety of aldehydes, including aromatic and fatty aldehydes. Two strong bands were visible in the native-PAGE gel when the fresh extracts of fresh PG of silkworm moths metabolized benzaldehyde and salicylaldehyde, suggesting either two types of BmAOX5 or another active form of BmAOX in the PG of female silkworm moths; these results were similar to those reported for *D. melanogaster* (Marelja et al. 2014). Only one strong

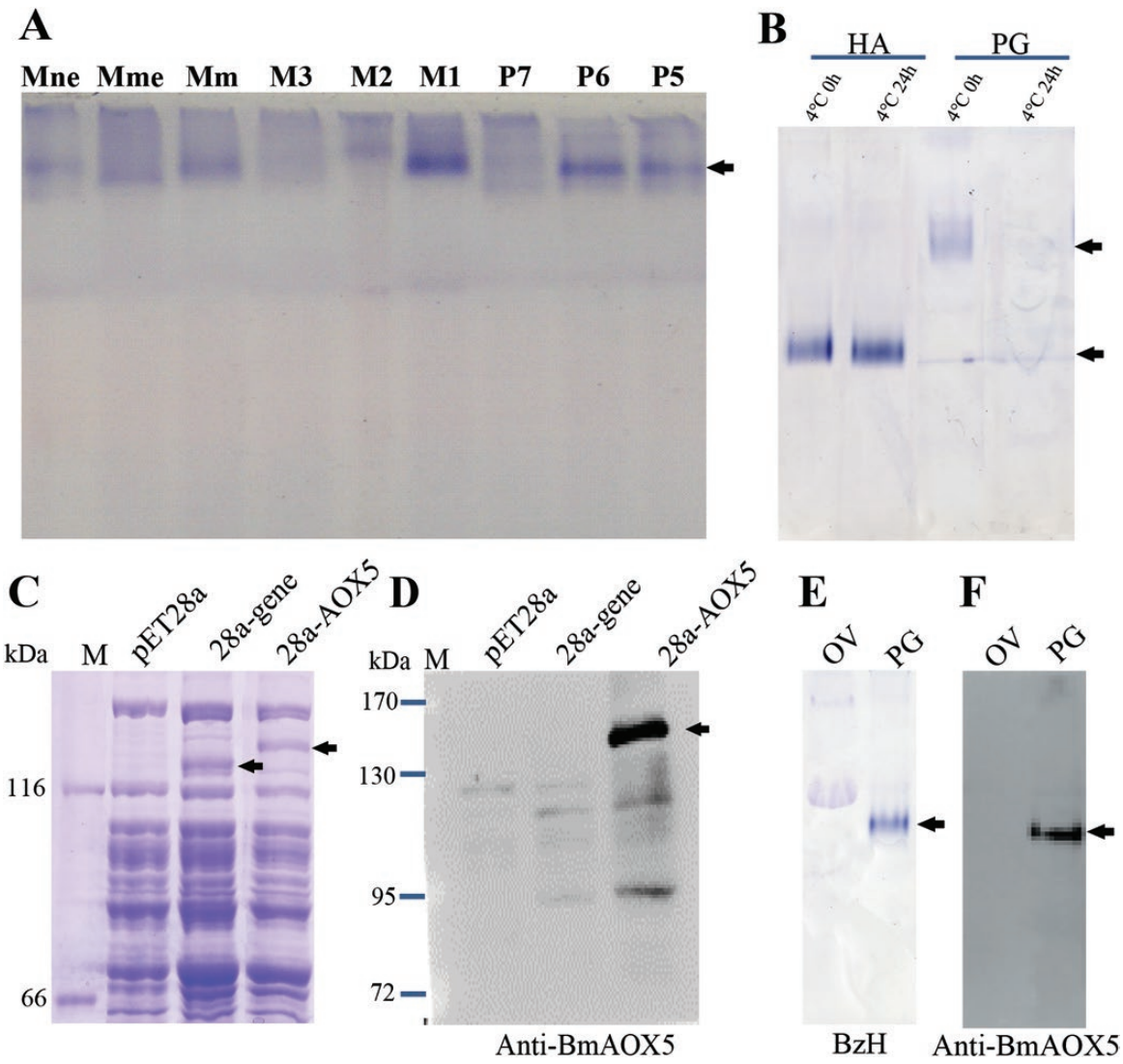

Fig. 3. Activity determination of BmAOX5 in silkworm PG. (A) Detection of AOX proteins in silkworm PG during different stages by native-PAGE and activity staining. Mne, moth after egg laying without mating; Mme, moth after egg laying with mating; Mm, moth after mating without egg laying; M3, moth day 3 without mating; M2, moth day 2 without mating; M1, moth day 1 without mating; P7, pupa day 7; P6, pupa day 6; P5, pupa day 5. (B) Stability detection of BmAOX in the PG by native-PAGE and activity staining. HA, antenna; PG, pheromone gland (including ovipositor). (C) Detection of BmAOX5 overexpressed in *E. coli* by SDS–PAGE and CBB staining. (D) Identification of BmAOX5 antibody by SDS–PAGE and western-blotting. M, standard protein marker; pET28a, extracts of *E. coli* transformed with pET28a empty vector as control; 28a-gene, extracts of *E. coli* transformed with pET28a vector with overexpression of another *BmAOX* gene as control; 28a-AOX5, extracts of *E. coli* transformed with pET28a vector with overexpression of *BmAOX5* gene. (E) Activity identification of BmAOX5 in the PG by native-PAGE and activity staining. (F) Protein identification of BmAOX5 by native-PAGE and western-blotting. OV, ovaries as control. Samples for B, E, F were tissues of female silkworm moth day 1 without mating and stored at –80°C before extracting proteins.

band was observed in metabolized heptaldehyde on the native-PAGE gel. These results revealed that the different AOXs are identified by different substrates.

Besides using native in-gel activity staining, we employed enzyme kinetics to measure BmAOX activity. As a substrate, benzaldehyde exhibited an activity band that corresponded with anti-BmAOX5 detection in the fresh extracts of frozen PG of silkworm moths. Thus, we selected fresh extracts of frozen PG of silkworm moths from day 1 without mating to measure BmAOX5 parameters using benzaldehyde as a substrate. The substrate saturation curve and Michaelis–Menten equation curve of the BmAOX5 catalytic reaction showed that BmAOX5 has typical characteristics of enzyme activity.

The PG, located between the eighth and ninth abdominal segments of the female silkworm moth, is an important organ for insect mating and oviposition (Tillman et al. 1999). It produces and releases sex pheromones, including bombykol (E-10, Z-12-hexadecadien-1-ol or BOL) and bombykal (E-10, Z-12-hexadecadien-1-al or BAL) (Butenandt et al. 1959, Kaissling et al. 1978, Tillman et al. 1999). BAL is a polyunsaturated, long-chain fatty aldehyde. We speculated BAL is metabolized also by BmAOX5 in the silkworm PG because BmAOX5 could metabolize fatty aldehydes such as heptaldehyde and propionaldehyde. Besides fatty aldehydes, BmAOX5 could metabolize aromatic aldehydes such as benzaldehyde, salicylaldehyde, and vanillic aldehyde. Recent studies have shown that the expression of 11 odorant-degrading enzyme genes is also found in the PG of *Eogystia hippophaec* by the transcriptome (Hu et al. 2020). Therefore, BmAOX5 may also metabolize other aldehydes in the cytoplasm for detoxification, or may participate in the degradation of aldehyde odorant

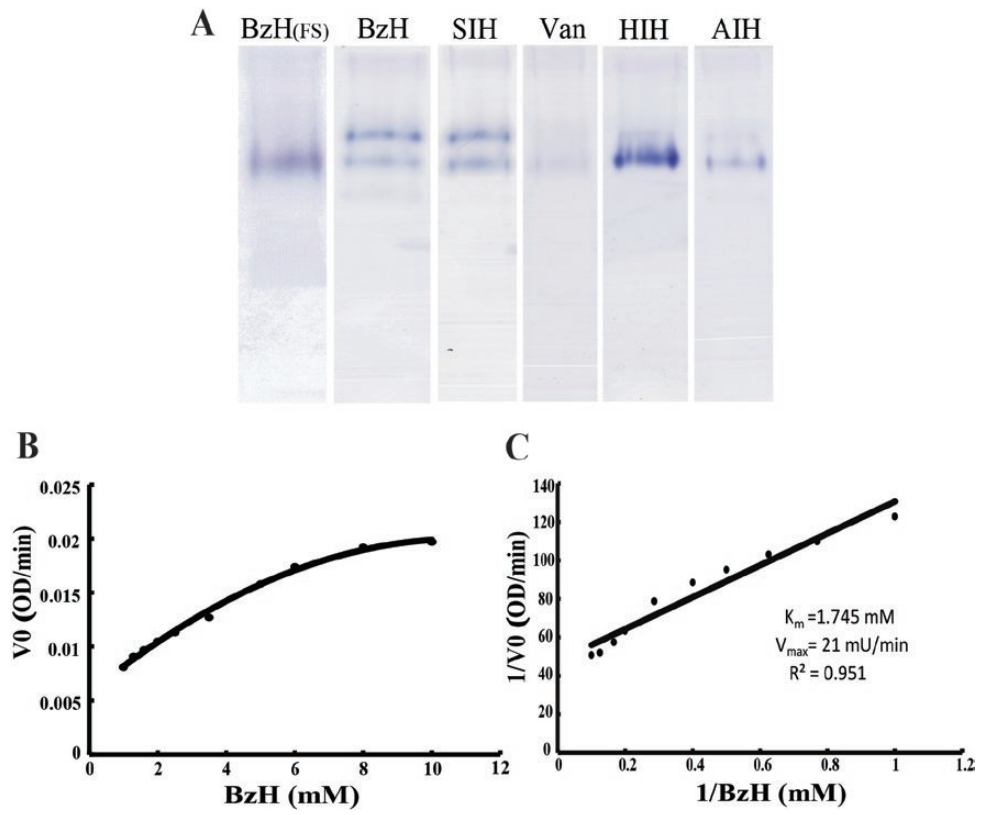

Fig. 4. Activity detection and enzymatic reaction kinetic analysis of BmAOX5. (A) Activity detection of BmAOX5 with different substrates by native-PAGE and AOX activity staining. BzH, benzaldehyde; SIH, salicylaldehyde; Van, vanillic aldehyde; HIH, heptaldehyde; AIH, propionaldehyde; FS, frozen PG. If FS is not marked, it means the PG was fresh, not stored in low temperature. (B) Enzymatic reaction curve of BmAOX5 substrate saturation. (C) Michaelis–Menten equation graph of BmAOX5 catalytic reaction with benzaldehyde as substrate. The formation of insoluble MTT formazan was measured at 560 nm. One OD/min representatives 1 unit of enzyme activity (1U), in the process of catalytic reaction. The concentration of benzaldehyde as a substrate follows: 1, 1.3, 1.6, 2, 2.5, 3.5, 5, 6, 8, and 10 mmol/liter. The OD value of each concentration is the average value of three independent experiments.

compounds to locate suitable and safe spawning sites (Choo et al. 2013, Marelja et al. 2014, Xu and Liao 2017).

Insects, similar to vertebrates (Qiao et al. 2020), have multiple copies of AOX genes. These genes express and synthesize active enzymes at different stages and in different tissues and metabolize various specific substrates. The purple stem borer, *Sesamia inferens*, has three AOX genes (Zhang et al. 2014). *D. melanogaster* has four AOX genes, among which DmAOX1, DmAOX2, and DmAOX3 can synthesize active enzymes and could metabolize multiple substrates including benzaldehyde and salicylaldehyde (Marelja et al. 2014). The silkworm has eight AOX genes (Pelletier et al. 2007, Yang et al. 2010), among which BmAOX1 and BmAOX2 are active in the antennae and mainly metabolize BAL secreted out by PG (Rybczynski et al. 1990, Pelletier et al. 2007); BmIAO1 is active in the silk gland, which is involved in indole-3-acetic acid synthesis (Takei et al. 2019). After a BLAST search for the reported N-terminal sequence STTKELTLKDGVKWFTVTQI of BmIAO1 (Takei et al. 2019) in the SilkDB2.0 and reported BmAOX sequences (Yang et al. 2010), we found that this protein should correspond to BmAOX7. Although the expression of BmAOX1 has been also found in the female silkworm PG (Pelletier et al. 2007, Yang et al. 2010), we did not detect BmAOX1 or BmAOX2 activity bands in silkworm moth PG extracts following in-gel of activity staining. This study demonstrated that BmAOX5 has activity in silkworm PG, and is able to metabolize multiple substrates such as DmAOXs (Marelja et al. 2014) and human AOX1 including vanillin, an edible flavor (Sahi et al. 2008), benzaldehyde, a sweetener (Garattini et al. 2008), in food. However, the other functions of these active AOXs have in insects is unknown. In particular, it is important to understand the structure–activity relationships of AOX binding and metabolism (Beedham et al. 1987, Dalvie et al. 2012, Coelho et al. 2015), species differences (Beedham et al. 1987, Terao et al. 2006, Dalvie et al. 2013), AOX variability (Terao et al. 2006, Adachi et al. 2007, Hutzler et al. 2014, Choughule et al. 2015), and in vitro activity of AOX (Stell et al. 1989, Alfaro et al. 2009, Liu et al. 2009). Silkworm has many types of AOXs. A clear understanding of their metabolic function could help in the preliminary detection and screening of drugs that are not metabolized by AOXs. Identifying a drug that can be metabolized by AOXs in the silkworm can provide a reference for animal medicinal research. Studies have also shown that silkworm can be used as an animal model for medical screening and studying disease mechanisms (Tabunoki et al. 2013, Paudel et al. 2020). The results of the present study on silkworm will help provide insight into the ecological control of pests and, at the same time, lay a theoretical foundation for an insect model that could be used for medical drug screening.

Acknowledgments

This work was supported by the State Key Program of National Natural Science of China (No. 32030103); the Fundamental Research Funds for the Central Universities (No. XDJK2017B006); and the National Natural Science Foundation of China (No. 31872429).

References Cited

Adachi, M., K. Itoh, A. Masubuchi, N. Watanabe, and Y. Tanaka. 2007. Construction and expression of mutant cDNAs responsible for genetic polymorphism in aldehyde oxidase in Donryu strain rats. J. Biochem. Mol. Biol. 40: 1021–1027.

Alfaro, J. F., C. A. Joswig-Jones, W. Ouyang, J. Nichols, G. J. Crouch, and J. P. Jones. 2009. Purification and mechanism of human aldehyde oxidase expressed in *Escherichia coli*. Drug Metab. Dispos. 37: 2393–2398.

Alirezaei, M., W. B. Kiosses, C. T. Flynn, N. R. Brady, and H. S. Fox. 2008. Disruption of neuronal autophagy by infected microglia results in neurodegeneration. PLoS One 3: e2906.

Badwey, J. A., J. M. Robinson, M. J. Karnovsky, and M. L. Karnovsky. 1981. Superoxide production by an unusual aldehyde oxidase in guinea pig granulocytes. Characterization and cytochemical localization. J. Biol. Chem. 256: 3479–3486.

Beedham, C., S. E. Bruce, D. J. Critchley, Y. al-Tayib, and D. J. Rance. 1987. Species variation in hepatic aldehyde oxidase activity. Eur. J. Drug Metab. Pharmacokinet. 12: 307–310.

Butenandt, A., H. Beckman, D. Stamm, and E. Hecker. 1959. Uber den sexual-lockstoff des seidenspinners *Bombyx mori*. reindarstellung and konstitution z. Naturforsch. B. 14: 283–284.

Choo, Y. M., J. Pelletier, E. Atungulu, and W. S. Leal. 2013. Identification and characterization of an antennae-specific aldehyde oxidase from the navel orangeworm. PLoS One 8: e67794.

Choughule, K. V., C. A. Joswig-Jones, and J. P. Jones. 2015. Interspecies differences in the metabolism of methotrexate: an insight into the active site differences between human and rabbit aldehyde oxidase. Biochem. Pharmacol. 96: 288–295.

Coelho, C., A. Foti, T. Hartmann, T. Santos-Silva, S. Leimkühler, and M. J. Romão. 2015. Structural insights into xenobiotic and inhibitor binding to human aldehyde oxidase. Nat. Chem. Biol. 11: 779–783.

Crouch, R. D., R. D. Morrison, F. W. Byers, C. W. Lindsley, K. A. Emmitte, and J. S. Daniels. 2016. Evaluating the disposition of a mixed aldehyde oxidase/cytochrome p450 substrate in rats with attenuated p450 activity. Drug Metab. Dispos. 44: 1296–1303.

Dalvie, D., C. Zhang, W. Chen, T. Smolarek, R. S. Obach, and C. M. Loi. 2010. Cross-species comparison of the metabolism and excretion of zoniporide: contribution of aldehyde oxidase to interspecies differences. Drug Metab. Dispos. 38: 641–654.

Dalvie, D., H. Sun, C. Xiang, Q. Hu, Y. Jiang, and P. Kang. 2012. Effect of structural variation on aldehyde oxidase-catalyzed oxidation of zoniporide. Drug Metab. Dispos. 40: 1575–1587.

Dalvie, D., C. Xiang, P. Kang, and S. Zhou. 2013. Interspecies variation in the metabolism of zoniporide by aldehyde oxidase. Xenobiotica 43: 399–408.

Duan, J., R. Li, D. Cheng, W. Fan, X. Zha, T. Cheng, Y. Wu, J. Wang, K. Mita, Z. Xiang, et al. 2010. SilkDB v2.0: a platform for silkworm (*Bombyx mori*) genome biology. Nucleic Acids Res. 38: D453–D456.

Enroth, C., B. T. Eger, K. Okamoto, T. Nishino, T. Nishino, and E. F. Pai. 2000. Crystal structures of bovine milk xanthine dehydrogenase and xanthine oxidase: structure-based mechanism of conversion. Proc. Natl. Acad. Sci. USA 97: 10723–10728.

Fónagy, A., N. Yokoyama, and S. Matsumoto. 2001. Physiological status and change of cytoplasmic lipid droplets in the pheromone-producing cells of the silkmoth, *Bombyx mori* (Lepidoptera, Bombycidae). Arthropod Struct. Dev. 30: 113–123.

Garattini, E., and M. Terao. 2013. Aldehyde oxidase and its importance in novel drug discovery: present and future challenges. Expert Opin. Drug Discov. 8: 641–654.

Garattini, E., R. Mendel, M. J. Romão, R. Wright, and M. Terao. 2003. Mammalian molybdo-flavoenzymes, an expanding family of proteins: structure, genetics, regulation, function and pathophysiology. Biochem. J. 372: 15–32.

Garattini, E., M. Fratelli, and M. Terao. 2008. Mammalian aldehyde oxidases: genetics, evolution and biochemistry. Cell. Mol. Life Sci. 65: 1019–1048.

Hall, T. A. 1999. Bioedit: a user-friendly biological sequence alignment editor and analysis program for windows 95/98/NT. Nucleic Acids Symposium Series: 95–98.

Hemingway, J., M. Coleman, M. Paton, L. McCarroll, A. Vaughan, and D. Desilva. 2000. Aldehyde oxidase is coamplified with the World's most common Culex mosquito insecticide resistance-associated esterases. Insect Mol. Biol. 9: 93–99.

Hu, P., D. Wang, C. Gao, P. Lu, J. Tao, and Y. Luo. 2020. Pheromone biosynthetic pathway and chemoreception proteins in sex pheromone gland of *Eogystia hippophaecolus*. Comp. Biochem. Physiol. Part D. Genomics Proteomics 35: 100702.

Hutzler, J. M., R. S. Obach, D. Dalvie, and M. A. Zientek. 2013. Strategies for a comprehensive understanding of metabolism by aldehyde oxidase. Expert Opin. Drug Metab. Toxicol. 9: 153–168.

Hutzler, J. M., Y. S. Yang, C. Brown, S. Heyward, and T. Moeller. 2014. Aldehyde oxidase activity in donor-matched fresh and cryopreserved human hepatocytes and assessment of variability in 75 donors. Drug Metab. Dispos. 42: 1090–1097.

Johnson, C., C. Stubley-Beedham, and J. G. Stell. 1985. Hydralazine: a potent inhibitor of aldehyde oxidase activity in vitro and in vivo. Biochem. Pharmacol. 34: 4251–4256.

Kaissling, K. E., G. Kasang, H. J. Bestmann, W. Stransky, and O. Vostrowsky. 1978. A new pheromone of the silkworm moth *Bombyx mori*. Sci. Nat. 65: 382–384.

Kitamura, S., K. Sugihara, and S. Ohta. 2006. Drug-metabolizing ability of molybdenum hydroxylases. Drug Metab Pharmacokinet. 21: 83–98.

Kundu, T. K., R. Hille, M. Velayutham, and J. L. Zweier. 2007. Characterization of superoxide production from aldehyde oxidase: an important source of oxidants in biological tissues. Arch. Biochem. Biophys. 460: 113–121.

Kurosaki, M., S. Zanotta, M. Li Calzi, E. Garattini, and M. Terao. 1996. Expression of xanthine oxidoreductase in mouse mammary epithelium during pregnancy and lactation: regulation of gene expression by glucocorticoids and prolactin. Biochem. J. 319(Pt 3): 801–810.

Laemmli, U. K. 1970. Cleavage of structural proteins during the assembly of the head of bacteriophage T4. Nature 227: 680–685.

Liu, P., S. Liang, B. J. Wang, and R. C. Guo. 2009. Construction of expression system of rabbit aldehyde oxidase cDNA for the clarification of species differences. Eur. J. Drug Metab. Pharmacokinet. 34: 205–211.

Mahro, M., C. Coelho, J. Trincão, D. Rodrigues, M. Terao, E. Garattini, M. Saggu, F. Lendzian, P. Hildebrandt, M. J. Romão, et al. 2011. Characterization and crystallization of mouse aldehyde oxidase 3: from mouse liver to Escherichia coli heterologous protein expression. Drug Metab. Dispos. 39: 1939–1945.

Majkic-Singh, N., B. Conteh, M. Stojanov, and I. Berkes. 1983. Kinetic assay of aldehyde oxidase with 2,2'-azino-di-(3-ethylbenzthiazoline-6-sulfonate) as chromogen. Enzyme 29: 120–125.

Marelja, Z., M. Dambowsky, M. Bolis, M. L. Georgiou, E. Garattini, F. Missirlis, and S. Leimkühler. 2014. The four aldehyde oxidases of *Drosophila melanogaster* have different gene expression patterns and enzyme substrate specificities. J. Exp. Biol. 217: 2201–2211.

Merlin, C., M. C. François, F. Bozzolan, J. Pelletier, E. Jacquin-Joly, and M. Maïbèche-Coisne. 2005. A new aldehyde oxidase selectively expressed in chemosensory organs of insects. Biochem. Biophys. Res. Commun. 332: 4–10.

Mira, L., L. Maia, L. Barreira, and C. F. Manso. 1995. Evidence for free radical generation due to NADH oxidation by aldehyde oxidase during ethanol metabolism. Arch. Biochem. Biophys. 318: 53–58.

Obach, R. S., P. Huynh, M. C. Allen, and C. Beedham. 2004. Human liver aldehyde oxidase: inhibition by 239 drugs. J. Clin. Pharmacol. 44: 7–19.

Panoutsopoulos, G. I., and C. Beedham. 2004. Kinetics and specificity of guinea pig liver aldehyde oxidase and bovine milk xanthine oxidase towards substituted benzaldehydes. Acta Biochim. Pol. 51: 649–663.

Paudel, A., S. Panthee, H. Hamamoto, and K. Sekimizu. 2020. A simple artificial diet available for research of silkworm disease models. Drug Discov. Ther. 14: 177–180.

Pelletier, J., F. Bozzolan, M. Solvar, M. C. François, E. Jacquin-Joly, and M. Maïbèche-Coisne. 2007. Identification of candidate aldehyde oxidases from the silkworm *Bombyx mori* potentially involved in antennal pheromone degradation. Gene 404: 31–40.

Petersen, T. N., S. Brunak, G. von Heijne, and H. Nielsen. 2011. SignalP 4.0: discriminating signal peptides from transmembrane regions. Nat. Methods 8: 785–786.

Pryde, D. C., D. Dalvie, Q. Hu, P. Jones, R. S. Obach, and T. D. Tran. 2010. Aldehyde oxidase: an enzyme of emerging importance in drug discovery. J. Med. Chem. 53: 8441–8460.

Qiao, Y., K. Maiti, Z. Sultana, L. Fu, and R. Smith. 2020. Inhibition of vertebrate aldehyde oxidase as a therapeutic treatment for cancer, obesity, aging and amyotrophic lateral sclerosis. Eur. J. Med. Chem. 187: 111948.

Rothe, G. M. 1974. Aldehyde oxidase isoenzymes (E.C. 1.2.3.1) in potato tubers (Solanum tuberosum). Plant Cell Physiol. 15: 493–499.

Rybczynski, R., J. Reagan, and M. R. Lerner. 1989. A pheromone-degrading aldehyde oxidase in the antennae of the moth *Manduca sexta*. J. Neurosci. 9: 1341–1353.

Rybczynski, R., R. G. Vogt, and M. R. Lerner. 1990. Antennal-specific pheromone-degrading aldehyde oxidases from the moths *Antheraea polyphemus* and *Bombyx mori*. J. Biol. Chem. 265: 19712–19715.

Sahi, J., K. K. Khan, and C. B. Black. 2008. Aldehyde oxidase activity and inhibition in hepatocytes and cytosolic fractions from mouse, rat, monkey and human. Drug Metab. Lett. 2: 176–183.

Stell, J. G., A. J. Warne, and C. Lee-Woolley. 1989. Purification of rabbit liver aldehyde oxidase by affinity chromatography on benzamidine sepharose 6B. J. Chromatogr. 475: 363–372.

Strelevitz, T. J., C. C. Orozco, and R. S. Obach. 2012. Hydralazine as a selective probe inactivator of aldehyde oxidase in human hepatocytes: estimation of the contribution of aldehyde oxidase to metabolic clearance. Drug Metab. Dispos. 40: 1441–1448.

Tabunoki, H., H. Ono, H. Ode, K. Ishikawa, N. Kawana, Y. Banno, T. Shimada, Y. Nakamura, K. Yamamoto, J. Satoh, et al. 2013. Identification of key uric acid synthesis pathway in a unique mutant silkworm *Bombyx mori* model of Parkinson's disease. PLoS One 8: e69130.

Takei, M., S. Kogure, C. Yokoyama, Y. Kouzuma, and Y. Suzuki. 2019. Identification of an aldehyde oxidase involved in indole-3-acetic acid synthesis in *Bombyx mori* silk gland. Biosci. Biotechnol. Biochem. 83: 129–136.

Terao, M., M. Kurosaki, M. Marini, M. A. Vanoni, G. Saltini, V. Bonetto, A. Bastone, C. Federico, S. Saccone, R. Fanelli, et al. 2001. Purification of the aldehyde oxidase homolog 1 (AOH1) protein and cloning of the AOH1 and aldehyde oxidase homolog 2 (AOH2) genes. Identification of a novel molybdo-flavoprotein gene cluster on mouse chromosome 1. J. Biol. Chem. 276: 46347–46363.

Terao, M., M. Kurosaki, M. M. Barzago, E. Varasano, A. Boldetti, A. Bastone, M. Fratelli, and E. Garattini. 2006. Avian and canine aldehyde oxidases. Novel insights into the biology and evolution of molybdo-flavoenzymes. J. Biol. Chem. 281: 19748–19761.

Terao, M., M. Kurosaki, M. M. Barzago, M. Fratelli, R. Bagnati, A. Bastone, C. Giudice, E. Scanziani, A. Mancuso, C. Tiveron, et al. 2009. Role of the molybdoflavoenzyme aldehyde oxidase homolog 2 in the biosynthesis of retinoic acid: generation and characterization of a knockout mouse. Mol. Cell. Biol. 29: 357–377.

Tillman, J. A., S. J. Seybold, R. A. Jurenka, and G. J. Blomquist. 1999. Insect pheromones–an overview of biosynthesis and endocrine regulation. Insect Biochem. Mol. Biol. 29: 481–514.

Walker-Simmons, M., D. A. Kudrna, and R. L. Warner. 1989. Reduced accumulation of ABA during water stress in a molybdenum cofactor mutant of barley. Plant Physiol. 90: 728–733.

Xia, Q., Z. Zhou, C. Lu, D. Cheng, F. Dai, B. Li, P. Zhao, X. Zha, T. Cheng, C. Chai, et al.; Biology Analysis Group. **2004**. A draft sequence for the genome of the domesticated silkworm (*Bombyx mori*). Science 306: 1937–1940.

Xu, W., and Y. Liao. 2017. Identification and characterization of aldehyde oxidases (AOXs) in the cotton bollworm. Naturwissenschaften. 104: 94.

Yang, Y., Y. Lin, C. W. Yang, Y. X. Wang, and Q. Y. Xia. 2010. Identification and expression profiling of aldehyde oxidase genes in the silkworm, *Bombyx mori*. Acta Entomologica Sinica. 53: 1–8.

Zhang, Y. N., Y. H. Xia, J. Y. Zhu, S. Y. Li, and S. L. Dong. 2014. Putative pathway of sex pheromone biosynthesis and degradation by expression patterns of genes identified from female pheromone gland and adult antenna of *Sesamia inferens* (Walker). J Chem Ecol. 40: 439–451.